

## Selective Guest Encapsulation by a Cobalt-Assembled Cage Molecule

Roger G. Harrison,\* Jessica L. Burrows, and Lee D. Hansen<sup>[a]</sup>

**Abstract:** Metal-assembled resorcinarene-based cages enclose space and entrap organic molecules from water. Addition of cobalt(II) ions to a neutral, aqueous solution of a resorcinarene that has iminodiacetic acids attached to its upper rim results in the formation of cages. These cages not only entrap organic molecules, but they do so in a selective manner. Guests with optimum size, shape, and polarity are preferentially entrapped. For example, selection

of *p*-xylene is twenty thousand times more favorable than that of *m*-xylene. The enthalpy of resorcinarene deprotonation and cage formation was calculated by performing calorimetry studies and ranged from  $-305$  to

**Keywords:** cage compounds • entropy of encapsulation • host–guest systems • molecular recognition • resorcinarenes

$-348$  kJ mol<sup>-1</sup>. The change in enthalpy of guest encapsulation varied by as much as 43 kJ mol<sup>-1</sup>. The differences in change in free energy of guest encapsulation varied by  $-16$  kJ mol<sup>-1</sup>. The changes in enthalpy and free energy of guest encapsulation were used to calculate the changes in entropy, which ranged from  $-97$  to  $+37$  J mol<sup>-1</sup> K<sup>-1</sup>. An enthalpy–entropy compensation of guest encapsulation was observed.

### Introduction

Molecular recognition is the initial step in many reactions. Catalytic transformation of biomolecules, selective catalysis, and chiral catalysis rely on molecular differentiation. To enhance molecular recognition, host molecules have several interaction sites. Thus, rings, cavitands, and cages, which have several binding sites that act in a cooperative manner, are used as hosts for selective molecular recognition. Over the last three decades, rings and cavitands with open frameworks have been used extensively to bind charged and neutral species.<sup>[1]</sup> Cage compounds, formed either by covalent, hydrogen, or metal bonds, have also been shown to exhibit strong molecular binding and encapsulation.<sup>[2]</sup>

Cages assembled with metal ions have a range of cavity sizes and encapsulate a variety of molecules.<sup>[3]</sup> Most enclose space by using metal ions to assemble several multidentate ligands. Many of the metal-assembled cages encapsulate either anions<sup>[4]</sup> or cations,<sup>[5]</sup> due to the overall charge on the cages being either positive because of the metal ions, or neg-

ative because of the ligands. Some also encapsulate neutral molecules, often of solvent.<sup>[6]</sup> One family of these metal-assembled cages consists of resorcinarene cavitands assembled by metal ions.<sup>[7]</sup> Resorcinarenes have preformed cavities of aromatic groups, which become walls in the cage when the resorcinarenes are grouped together by the metal ions. We have found that resorcinarene-based metal-assembled cages are able to encapsulate a variety of neutral organic molecules containing aliphatic, aromatic, and heteroatom moieties.<sup>[8]</sup> The resorcinarene-based metal-ion-assembled cages are similar to the organic and hydrogen-bonded resorcinarene-based molecules that have an extensive history of encapsulation. The metal-ion-assembled cages differ, however, in that they are assembled and soluble in water, their encapsulation is triggered by pH change, and they have metal ions close to the encapsulated guest molecules. These cages may, therefore, be useful for the removal of organic molecules from water, in catalyzing the reactivity of encapsulated guests, and as NMR shift reagents.

Although guest encapsulation is mediated by most cages, the selective encapsulation of a guest is more challenging. Selective guest encapsulation is important for separating similar molecules or for encapsulating a specific target molecule. In the formation of organic-based<sup>[9]</sup> and hydrogen-bonded<sup>[10]</sup> cages, the guest often acts as a template for cage formation, and the template effect can be very dramatic. The template-directed assembly of metal cages has also been reported.<sup>[11]</sup> Although selective encapsulation is well

[a] Prof. R. G. Harrison, J. L. Burrows, Prof. L. D. Hansen  
Department of Chemistry and Biochemistry  
Brigham Young University, Provo, Utah 84602 (USA)  
Fax: (+1) 801-422-0153  
E-mail: roger\_harrison@byu.edu

established in nonmetal-assembled cages,<sup>[12]</sup> it is rare in metal-assembled cages.<sup>[13]</sup> Here, we present detailed findings on the selective encapsulation of organic molecules by metal-assembled cages.

We previously found that the assembly of resorcinarenes with appended iminodiacetate groups into cage molecules can be induced by metal ions, and that these metal-assembled cages can encapsulate organic molecules.<sup>[8]</sup> Thus, the addition of cobalt(II) or iron(II) ions to a solution of functionalized resorcinarene (**1**) and organic molecules results in the encapsulation of the organic molecules by the metal-resorcinarene cage. Guest encapsulation can be demonstrated by a large upfield shift in the NMR spectrum of the encapsulated guest (30 ppm), and by X-ray crystallography showing guest molecules in the cage. Even though these metal-assembled cages are water soluble because of their overall anionic charge, they possess an elliptical (10×11 Å), hydrophobic cavity surrounded by aryl and etheric groups. In addition, we were able to show that the cages encapsulate guests selectively. For example, *p*-xylene is encapsulated twenty thousand times more favorably than either *o*- or *m*-xylene. The encapsulation preference correlates with the size, shape, and polarity of the guest. The enthalpy change during encapsulation is favorable for the highly selected guests. Calorimetric titrations show that several steps are involved in cage formation and guest encapsulation. Differences in free energy and entropy changes for guest encapsulation were calculated from competitive encapsulation ratios and the enthalpies of encapsulation.

## Results

Stirring of the resorcinarene-based cavitand (**1**), cobalt(II) ions, and organic molecules at pH > 5 results in the formation of cage molecules ( $[\text{Co}_4(\mathbf{1})_2]^{8-}$ ) and the encapsulation of organic molecules (Scheme 1). This occurs in most cases, even though the organic molecules are present at a lower concentration than the water molecules, with which they compete for the cage interior. To determine the preference of a cage for one guest over another, studies were performed in which two different organic molecules were pres-

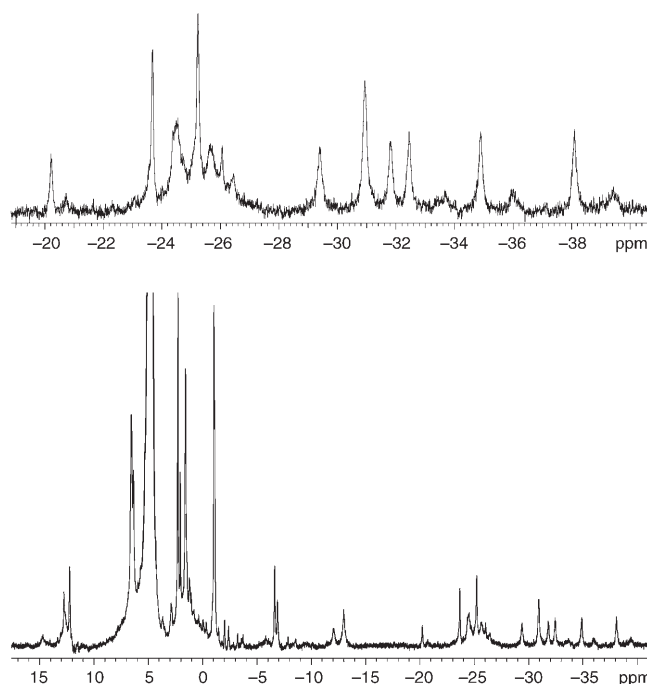
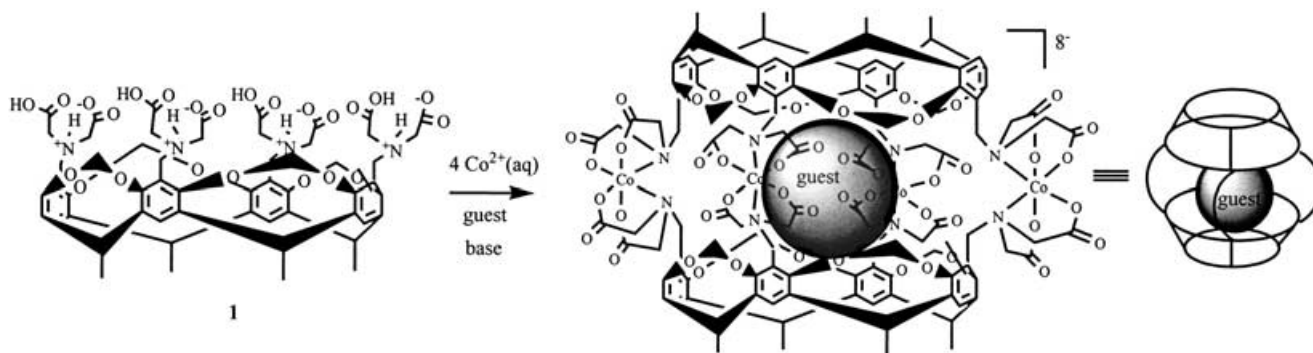


Figure 1. <sup>1</sup>H NMR spectra of a cage formed in the presence of toluene and *n*-hexane. Bottom spectrum shows cage peaks and guest peaks from 20 to -40 ppm. Top spectrum is a blow up of the -20 to -40 ppm region. There are two sets of cage peaks, one with toluene inside and one with hexane inside. The cage peaks are at -24.5, -25.5, -31, and -32 ppm. The four peaks for encapsulated toluene are at -20, -23.5, -29, and -32.5 ppm. The three peaks for hexane are at -25, -35, and -38 ppm. (The small broad peaks next to the hexane peaks are for a minor isomer.)

ent during cage formation. As shown in Figure 1, the proton resonances of the encapsulated guests appear in the -20 to -40 ppm region of an NMR spectrum. The proton NMR signals were integrated to obtain the quantity of each cage-guest complex. The cage has a high affinity for some molecules (e.g., anisole and *p*-xylene) and a low affinity for others (e.g., pentane and dichloromethane), as seen in Table 1. The values listed in Table 1 are the selectivities relative to that of benzene, which was set at 100.



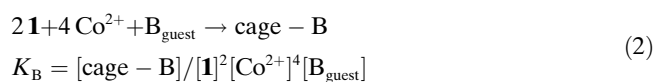
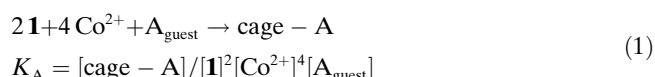
Scheme 1. Guest encapsulation by a metal-assembled cage.

Table 1. Relative guest encapsulation preference.<sup>[a]</sup>

Guest (solubility in mmol L <sup>-1</sup> H <sub>2</sub> O at 25 °C) <sup>[19]</sup>	Encapsulation preference
anisole	27 400
<i>p</i> -xylene (1.7)	26 700
ethyl benzene (1.5)	2700
acetonitrile <sup>[b]</sup>	1050
ethyl acetate (920)	800
toluene (5.9)	600
styrene	580
4-chlorotoluene	430
bromobenzene (2.9)	390
1-isoamyl alcohol (410)	270
1-hexanol (52)	210
hexane (0.13)	206
diethyl ether (810)	200
1-bromobutane	170
1-pentanol (240)	122
heptane (0.023)	105
1-chlorobutane	103
chlorobenzene (4.35)	102
benzene (23)	100
1-butanol (1100)	96
1,2-dibromoethane	80
1-bromopropane (19)	77
benzonitrile	69
1-bromopentane	67
fluorobenzene (16)	42
pentane (0.58)	40
bromoethane	35
chloroform (84)	18
1,2-dichloroethane (88)	7
dichloromethane (235)	3
tetrahydrofuran	2
<i>m</i> -xylene (1.7)	<1
<i>o</i> -xylene (1.7)	<1

[a] Values are the selectivities relative to that of benzene, which was set at 100. [b] Two guest molecules were encapsulated.

Relative selectivity values can be used to calculate relative free energy changes for guest encapsulation. In the presence of two potential guest molecules, the reactions are:



Because  $[\mathbf{1}]$  and  $[\text{Co}^{2+}]$  were kept constant, Equation (1) can be divided by Equation (2) to give the expression  $([\text{cage} - \text{A}] / [\text{cage} - \text{B}]) / ([\text{A}_{\text{guest}}] / [\text{B}_{\text{guest}}]) = K$ , in which  $K = K_{\text{A}} / K_{\text{B}}$ . The ratio of  $[\text{cage} - \text{A}] / [\text{cage} - \text{B}]$  is the same as the guest encapsulation preference. The ratio  $[\text{A}_{\text{guest}}] / [\text{B}_{\text{guest}}]$  is calculated by subtracting the amount of guest in the cage from the original amount of guest. From the relationship  $\Delta G^{\circ} = -RT \ln K$ , the difference in free energy of encapsulation between two guests can be calculated. For example, for toluene and benzene,  $\Delta G^{\circ} = -4.5 \text{ kJ mol}^{-1}$ ; for *p*-xylene and benzene,  $\Delta G^{\circ} = -14 \text{ kJ mol}^{-1}$ ; and for *p*-xylene and fluorobenzene,  $\Delta G^{\circ} = -16 \text{ kJ mol}^{-1}$ .

Results of NMR analysis to track cage formation and guest entrapment showed that at  $\text{pH} < 3.0$ , cavitand proton resonances are in the diamagnetic region and, thus, the cavitand is not bound to the paramagnetic  $\text{Co}^{2+}$  ions. As the pH exceeds a value of 3.0, the proton resonances broaden, which indicates the binding of  $\text{Co}^{2+}$  ions. At pH greater than 5.0, the cavitand proton signals become narrower and cover a range of 200 ppm, indicating that the metal-assembled cage has formed. There is not a clear change of proton NMR signals from metal-free cavitand to cage, due in part to the shifting of resonances from the diamagnetic to the paramagnetic region. Thus, equilibrium constants for guest encapsulation could not be determined by NMR analysis.

Titration calorimetry was used to measure the enthalpy change for encapsulation.<sup>[15]</sup> Initial titrations of  $\text{Co}^{2+}$  ions into a solution of  $\mathbf{1}^{8-}$  showed that the formation of a cage from two molecules of  $\mathbf{1}^{8-}$  and four  $\text{Co}^{2+}$  ions is kinetically controlled. Titration curves were complex and did not show the stoichiometry for quantitative cage formation. Results of NMR titrations showed that some of the iminodiacetate groups of  $\mathbf{1}^{8-}$  were not coordinated to  $\text{Co}^{2+}$ , even in the presence of excess  $\text{Co}^{2+}$  ions. The inverse titration, in which  $\mathbf{1}^{8-}$  was titrated into a solution of  $\text{Co}^{2+}$  ions, revealed the formation of several unidentified products before the appearance of the final  $[\text{Co}_4(\mathbf{1})_2]^{8-}$  product. To create a reaction environment similar to that used in the selective encapsulation studies, an acidic solution containing  $\mathbf{1}$  and  $\text{Co}^{2+}$  ions was titrated with a solution of NaOH. Quantitative formation of cage by this method was confirmed by performing NMR titrations. This indirect titration method requires correction for the heats of deprotonation and water formation, but allows determination of the heat of cage formation.

Following the titration of an acidic solution of  $\mathbf{1}$  with a base, two exothermic regions are noted (Figure 2). The enthalpy change for the first region is approximately  $-38 \text{ kJ}$  per mole of  $\text{OH}^-$  ions. The iminodiacetic acid moieties of  $\mathbf{1}$  can have three acidic protons; two on the carboxyl groups and one on the nitrogen atom. At pH 3.0, at which the initial titrations are performed, the iminodiacetic acid group has lost the hydrogen atom from one carboxyl group ( $\text{p}K_{\text{a}}$  less than 0) and most of the hydrogen atoms from the other carboxyl group ( $\text{p}K_{\text{a}} = 2.3$ ).<sup>[16]</sup> Thus, the first portion of added hydroxide reacts with ionized  $\text{H}^+$  ions and increases the dissociation of the second carboxyl group of the iminodiacetic acid groups (Scheme 2). As the mole ratio of added hydroxide increases from  $\approx 1.5$  to 5.5, the proton from the nitrogen of the iminodiacetic acid is removed. Curve fitting<sup>[17]</sup> the titration data produces a conditional equilibrium constant, associated with loss of the ammonium proton, of  $3.0 \times 10^5$ , assuming a one-site model. The enthalpy change for the second region is  $-29 \text{ kJ mol}^{-1}$ , which is similar to that calculated upon titration of the model compound, benzyliminodiacetic acid (BIDA), with  $\text{OH}^-$ ,  $K = 1.6 \times 10^5$  and  $\Delta H^{\circ} = -28 \text{ kJ mol}^{-1}$ . These data are in agreement with the literature values for BIDA ( $K = 1.3 \times 10^5$ ) and methyliminodiacetic acid ( $\Delta H^{\circ} = -29 \text{ kJ mol}^{-1}$ ).<sup>[16]</sup> The titration of BIDA was performed in the same way as for  $\mathbf{1}$ , except that the

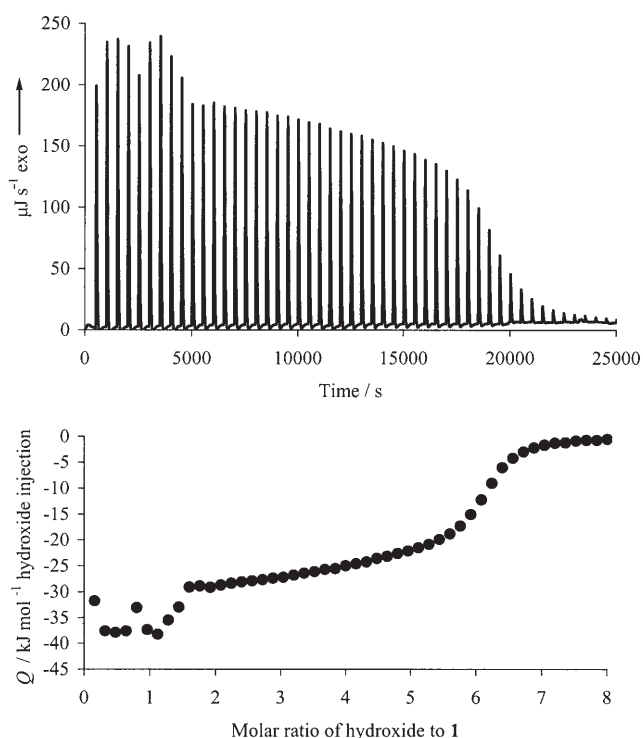
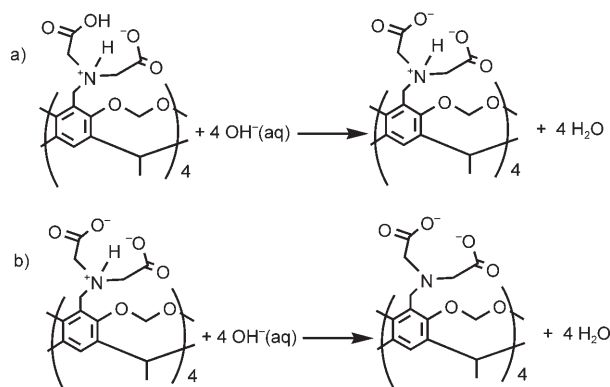


Figure 2. ITC titration curves, thermogram (top) and isotherm (bottom), for the titration of  $2.4 \mu\text{M}$  **1** with  $92 \text{ mM}$  NaOH.



Scheme 2. Deprotonation of **1**.

concentration of BIDA was four times that of **1**. Each molecule of **1** has four iminodiacetic acid groups and, therefore, the  $pK_a$  of one group could be affected by removal of a proton from another group. The distance between the iminodiacetic acid groups is too small for them to be independent of each other.

Titration of a solution of **1** with a base in the presence of  $\text{Co}^{2+}$  ions produces a more complex titration curve (Figure 3). During the titration, deprotonated **1**, cobalt-coordinated **1**, and cage are formed sequentially (Scheme 3). At the beginning of the titration (Figure 3, region a), at a pH of approximately 3.0, the heat corresponds to the reaction of

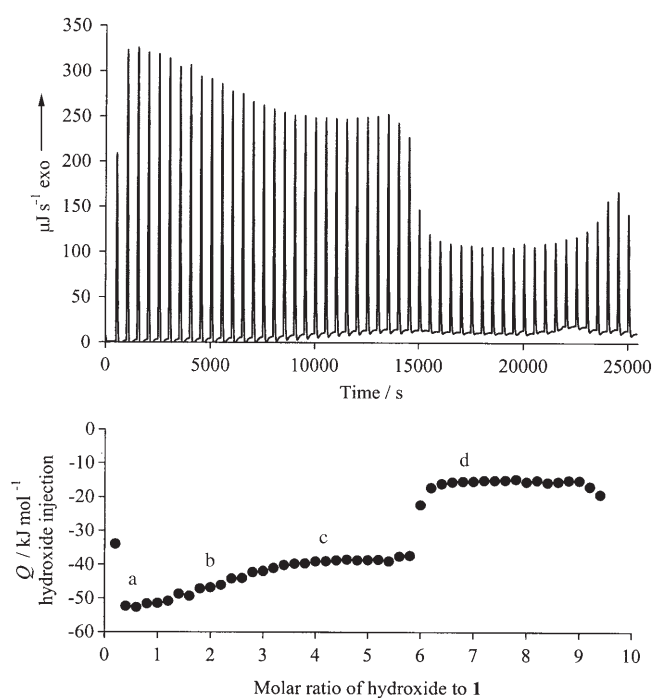
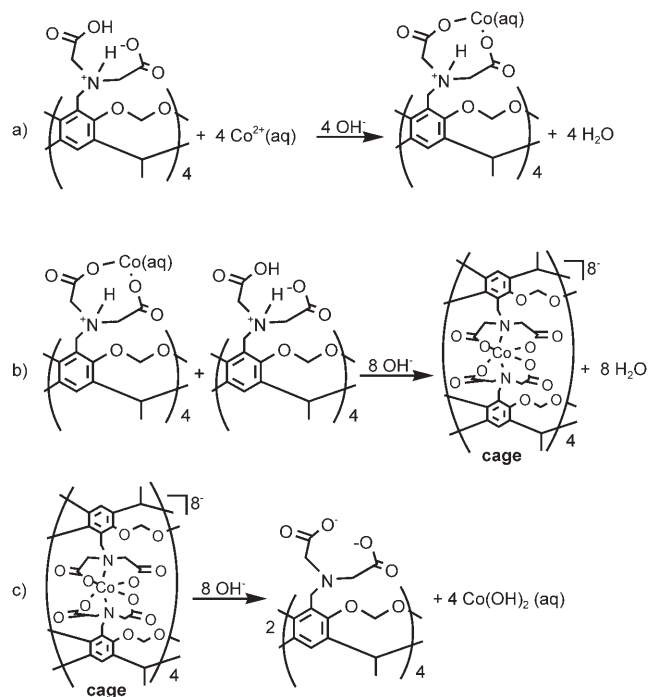


Figure 3. ITC titration curves, thermogram (top) and isotherm (bottom), for the titration of  $2.4 \mu\text{M}$  **1** and  $8.4 \mu\text{M}$   $\text{Co}^{2+}$  with  $92 \text{ mM}$  NaOH.



Scheme 3. Deprotonation,  $\text{Co}^{2+}$  coordination, and cage formation.

free protons and protonated carboxyl groups with  $\text{OH}^-$  ions, and the coordination of cobalt to carboxylate groups. This region gradually becomes less exothermic (region b), and indicates a situation in which protonated carboxyl, unbound  $\text{Co}^{2+}$  ions, carboxylate, and coordinated  $\text{Co}^{2+}$  ions are in

equilibrium. This phase (a–c) is followed by an exothermic region of constant heat evolution per injection (region c), which corresponds to nitrogen deprotonation and cage formation. There is then a sharp decrease in heat evolved per injection, followed by another region of constant heat per injection, in which blue cobalt hydroxide forms (region d). After this, the heat per injection equals the heat of dilution.

The stage of the titration at which one  $\text{Co}^{2+}$  ion coordinates to two iminodiacetate groups, thus bringing together two cavitands to form a cage, reveals a lot about cage assembly. Data from this stage is expected to be influenced by guest encapsulation. Titration of a solution of **1** and  $\text{Co}^{2+}$  ions in the presence of a guest produces curves similar to those obtained in the absence of a guest, except in the case of highly selected guests, such as anisole and *p*-xylene. In the presence of these guests, a constant heat per injection is observed not only during cage formation (Figure 4), but also from the beginning of the titration to the point at which cobalt hydroxide forms, which shows that these guests favor cage formation.

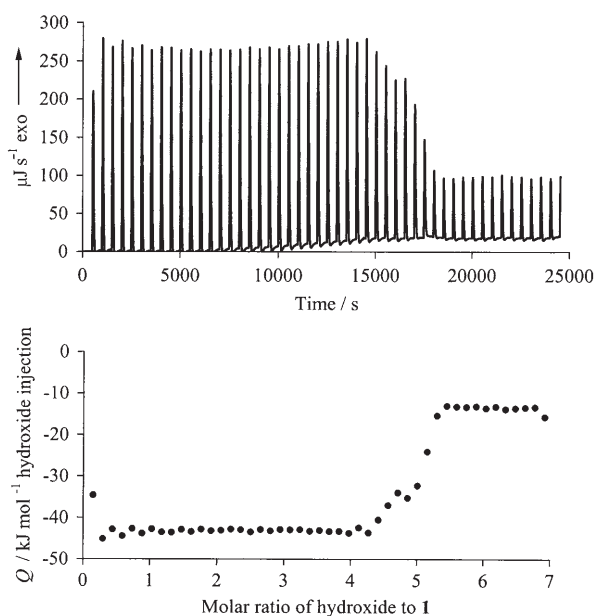


Figure 4. ITC titration curves, thermogram (top) and isotherm (bottom), for the titration of  $2.4 \mu\text{M}$  **1**,  $8.4 \mu\text{M}$   $\text{Co}^{2+}$ , and *p*-xylene with 92 mM NaOH.

The enthalpy change of cage formation can be calculated from the average heat during the constant exothermic region attributed to cage formation (region c of Figure 3). As Table 2 shows, the enthalpy change of cage formation is  $\approx -310 \text{ kJ mol}^{-1}$  for many guests and  $\approx -348 \text{ kJ mol}^{-1}$  for others. The enthalpy change of cage formation is apparently more exothermic for guests that are highly selected, such as *p*-xylene and anisole. Guests whose selectivity preferences are fairly similar, such as toluene, benzene, and ether, have similar enthalpy changes for cage formation.

Table 2. Heats of deprotonation, cobalt coordination, and cage formation.

Compounds in solution <sup>[a]</sup>	Heat <sup>[b]</sup> [kJ mol <sup>-1</sup> ]	Heat <sup>[c]</sup> [kJ mol <sup>-1</sup> ]	Heat <sup>[d]</sup> [kJ mol <sup>-1</sup> ]
BIDA	-27.6		
<b>1</b>	-28.5		
BIDA, $\text{Co}^{2+}$	-31.4	-62.8	
<b>1</b> , $\text{Co}^{2+}$	-38.5	-77.0	-308
<b>1</b> , $\text{Co}^{2+}$ , chloroform	-39.7	-79.4	-318
<b>1</b> , $\text{Co}^{2+}$ , fluorobenzene	-39.3	-78.6	-314
<b>1</b> , $\text{Co}^{2+}$ , benzene	-38.1	-76.2	-305
<b>1</b> , $\text{Co}^{2+}$ , diethyl ether	-38.5	-77.0	-308
<b>1</b> , $\text{Co}^{2+}$ , toluene	-39.3	-78.6	-314
<b>1</b> , $\text{Co}^{2+}$ , ethyl acetate	-38.1	-76.2	-305
<b>1</b> , $\text{Co}^{2+}$ , <i>p</i> -xylene	-43.5	-87.0	-348
<b>1</b> , $\text{Co}^{2+}$ , anisole	-43.5	-87.0	-348

[a] Guests listed in order of selectivity. [b] Per mol of base added. [c] Per  $[\text{Co}(\text{ida})_2]^{2-}$  formed. [d] Per cage formed.

## Discussion

To assist in the understanding of guest selectivity, a few properties of the cage need to be reviewed. The cage is ellipsoid in shape, being slightly larger in one direction than it is in the other. It has two poles that are rich in aromatic groups, with each pole being surrounded by four phenyl groups. The cage has an equator region surrounded by etheric groups that are slightly polar. The crystal structure of the cage shows that the metal ions and their amine and carboxylate ligands face away from the internal cavity of the cage.<sup>[8]</sup> The metal centers are around the equator of the cage and are separated from the cage's cavity by methylene groups.

The size of the cage's cavity is important to guest selectivity. Of the nonpolar aromatic compounds, *p*-xylene is preferred over toluene, which is preferred over benzene. This is explained by the methyl groups of xylene and toluene, which point into the poles of the cage and form C–H–aryl and van der Waal interactions. The two methyl groups of xylene form a stronger interaction than either the single methyl group of toluene or a hydrogen atom on benzene. The cage selectivity for benzene-containing molecules is explained by their optimum size. Seven of the ten most strongly encapsulated molecules contain a benzene ring. Although aromatic compounds are some of the most highly selected, they also show variations in selectivity. There is a correlation between size and encapsulation selectivity; for example, *p*-xylene (26700), ethyl benzene (2700), toluene (600), and benzene (100) show that encapsulation selectivity follows a trend from largest to smallest. Thus, the replacement of the hydrogen atoms on benzene with methyl groups increases the cage preference for a molecule. However, the cage does not encapsulate aromatic molecules that have more than two non-hydrogen atoms on a benzene ring.

A size effect is also demonstrated by the encapsulation of alkane and haloalkane. The cage has a preference for alkanes with intermediate chain lengths, as shown by the selec-

tion of *n*-hexane (206) over *n*-heptane (105) and *n*-pentane (40), and 1-bromobutane (170) over 1-bromopentane (67) and 1-bromopropane (77). Small molecules, such as chloroform, 1,2-dichloroethane, and methylene chloride are all poorly selected, due to both size and polarity. One exception was the small molecule, acetonitrile, which was encapsulated with preference to larger molecules. However, in contrast to all other molecules, two acetonitrile molecules were encapsulated instead of one.

The aromatic compounds also show that the shape of the cage cavity affects guest encapsulation. Molecules of *p*-xylene are selected twenty thousand times more readily than molecules of *o*- and *m*-xylene. In the *o*- and *m*-isomers of xylene, one methyl group is positioned at a cage pole, and the other methyl group is positioned close to the equator, forcing aryl hydrogen atoms to contact cage atoms. Another example of shape selectivity is shown by comparing ethyl benzene to styrene and benzonitrile. The *sp*<sup>3</sup> carbon atoms of the ethyl group on ethyl benzene make a favorable aryl–C–C bond angle (109°) to allow for increased interaction of a methyl group with the cage, whereas the *sp*<sup>2</sup> carbon atoms of styrene (aryl–C–C bond angle of 120°) and the *sp* carbon atoms of benzonitrile (aryl–C–N bond angle of 180°) form bond angles that do not allow for favorable methylene or nitrogen interactions.

The interaction between guest and cage polarity also affects guest encapsulation. The importance of guest polarity is demonstrated by the series in which bromobutane (170) is selected over chlorobutane (103) and pentane (40). As another example, *p*-xylene (26700) is favored over *p*-chlorotoluene (430), and toluene (600) is favored over chlorobenzene (102). Cases in which the larger and more polarizable bromine is bound to benzene show selectivities greater than those of the chlorine compounds. Bromobenzene is preferred over chlorobenzene, which is preferred over fluorobenzene. Although chlorobenzene is larger than benzene, it does not have an improved selectivity. Bromine-containing alkanes are selected over similar chlorine-containing compounds, as shown by the preference of bromobutane to chlorobutane (2:1 preference) and 1,2-dibromoethane to 1,2-dichloroethane (10:1 preference).

Heteroatom-containing compounds also reveal how guest polarity may enhance encapsulation. Anisole is preferred over ethyl benzene (10:1), diethyl ether over pentane (5:1), and 1-hexanol over heptane (2:1). Furthermore, polar molecules, such as acetonitrile, ethyl acetate, and 1-isoamyl alcohol, are towards the top of the selectivity list. This encapsulation of polar molecules exists even though their dipole attraction to the solvent water molecules is stronger than that of the nonpolar molecules. However, there is a limit to how polar a molecule can be and still be encapsulated. For example, encapsulation of water competes with the encapsulation of ethanol and is, in fact, preferred over the encapsulation of methanol and DMF. Under the encapsulation conditions, methanol and DMF are not detected in the cages. The enhanced acidity of the protons on the carbon next to the heteroatom may enhance the encapsulation of these molecules.

Another possible explanation for guest selectivity is that those compounds that are least soluble in water are trapped most easily. This explanation seems to be valid in a qualitative sense for some guests. For example, the solubility (mmol L<sup>-1</sup>) trend of benzene (23) > toluene (5.9) > ethylbenzene (1.5) ≈ *p*-xylene (1.7) is opposite to their trend in selectivity: *p*-xylene (26700) > ethylbenzene (2700) > toluene (600) > benzene (100). This explanation also seems plausible when considering that very polar molecules, such as acetone, methanol, and dimethylsulfoxide, are only sparingly encapsulated. However, not all compounds support this theory; for example, the trend in solubility (mmol L<sup>-1</sup>) for the following polar compounds is: ethyl acetate (920) > diethyl ether (810) > 1-pentanol (240) > chloroform (84), and yet, the trend in encapsulation preference is qualitatively the same: ethyl acetate (804) > diethyl ether (200) > 1-pentanol (122) > chloroform (18). Slightly soluble guests along with soluble guests are shown at the top and bottom of Table 1.

The difference in free energy calculated from the selectivity difference shows that those guests that are highly selected are thermodynamically favored by about 16 kJ mol<sup>-1</sup> (Table 3). This is similar to the difference in free energy be-

Table 3. Differences in the free energies, enthalpies, and entropies of encapsulation between guests.

Guests: preferred guest given first	$\Delta\Delta G^\circ$ [kJ mol <sup>-1</sup> ]	$\Delta\Delta H^\circ$ [kJ mol <sup>-1</sup> ]	Calcd $\Delta\Delta S^\circ$ [J mol <sup>-1</sup> K <sup>-1</sup> ]
benzene/fluorobenzene	-2.1	9.0	37
toluene/benzene	-4.5	-9.0	-15
<i>p</i> -xylene/toluene	-9.1	-34	-84
<i>p</i> -xylene/benzene	-14	-43	-97
<i>p</i> -xylene/fluorobenzene	-16	-34	-60

tween guests encapsulated by cryptophanes.<sup>[18]</sup> The difference in enthalpy can be calculated by using the heats of cage formation in the presence of different guests. These differences do not follow an orderly trend to more negative values in the way that the free energies do. By substituting the free energy differences and enthalpy differences into the Gibbs–Helmholtz equation,  $\Delta G^\circ = \Delta H^\circ - T\Delta S^\circ$ , the differences in entropy can be calculated (Table 3). The differences in entropy correlate well with the size of the guest. If the size difference between two guests is large, such as between *p*-xylene and benzene, the entropy change corresponding to encapsulation of the larger guest is more negative and less entropically favorable. However, if a smaller guest is encapsulated, such as benzene instead of fluorobenzene, the difference in entropy is positive. Therefore, both the enthalpy and entropy are important to guest selectivity. For example, comparison of benzene and fluorobenzene shows that the enthalpy of cage formation for benzene relative to fluorobenzene is positive (9.0 kJ mol<sup>-1</sup>) and enthalpically not favorable; however, the entropy is positive (37 J mol<sup>-1</sup> K<sup>-1</sup>) and favorable, which results in a preference for benzene encapsulation. Another example is shown by comparing *p*-xylene to benzene. The enthalpy of *p*-xylene encapsulation

is much more favorable ( $-43 \text{ kJ mol}^{-1}$ ) than that for benzene; however, the entropy is much less favorable ( $-100 \text{ J mol}^{-1} \text{ K}^{-1}$ ). The enthalpy–entropy compensation displayed by guest encapsulation is not uncommon for the binding of guest to synthetic or enzyme receptors.<sup>[19]</sup>

Along with the titration calorimetry experiments for **1**, the benzyliminodiacetic acid (BIDA) model compound, which is capable of forming a BIDA:Co coordination compound of ratio 2:1, but not capable of assembling into a cage, was also titrated. The heat of coordination of cobalt to two BIDA molecules is less exothermic than the heat of coordination of cobalt to two iminodiacetate units of **1** upon formation of a cage. Thus, even though the four iminodiacetate groups on each **1** could coordinate to cobalt ions and form other species apart from cages, such as oligomers, it is thermodynamically favorable by about  $8 \text{ kJ mol}^{-1}$  per cobalt ion for the iminodiacetate groups to assemble two molecules of **1** into a cage.

The last part of the titration, during which cobalt hydroxide forms, is similar for all of the titrations ( $\Delta H^\circ = -14 \text{ kJ mol}^{-1}$  of base) and does not show a correlation to the guest present. However, this heat was less exothermic when the cage was disassembled than when  $[\text{Co}(\text{bida})_2]$  was broken apart ( $\Delta H^\circ = -18 \text{ kJ mol}^{-1}$  of base). Breaking the bonds between four cobalt ions and eight iminodiacetate groups from the cage and the formation of a cobalt hydroxide species is less favorable than breaking the bonds between one cobalt and two BIDA molecules. As formation of the cage is more stable, it is less favorable to break it apart.

## Conclusion

The metal-assembled resorcinarene-based cage, **1**, selectively encapsulates neutral organic molecules. The most dominant factors in encapsulation selectivity are guest fit and polarity. The guest of optimum size, shape, and polarity for the cavity will occupy the greatest amount of cavity space and have the greatest number of favorable bonding interactions with the interior of the cage. Consequently, it will achieve optimum binding. In most cases, molecules with intermediate polarity are selected over those that are either nonpolar or very polar. The enthalpy changes for cage formation around guests differ by as much as  $43 \text{ kJ mol}^{-1}$  and the free energy changes for guest encapsulation range from 2 to  $15 \text{ kJ mol}^{-1}$ . For the encapsulated guests, the entropy changes range from  $-100$  to  $+37 \text{ J mol}^{-1} \text{ K}^{-1}$  and correlate to the differences in sizes of the guests.

## Experimental Section

Solvents, reagents, and organic compounds were used as supplied from commercial sources.  $[\text{Ba}_4(\mathbf{1})]$  was synthesized as previously described.<sup>[8]</sup>  $^1\text{H}$  NMR studies were performed by using a Varian INOVA 300 MHz Multinuclear FT-NMR spectrometer. Calorimetry was performed by using a Calorimetry Sciences Corp. Isothermal Titration Calorimeter Model 4209.

**Selectivity studies:**  $[\text{Ba}_4(\mathbf{1})]$  (100 mg,  $45 \mu\text{mol}$ ) was dissolved in water (7 mL) and 1 M HCl (2 mL).  $\text{K}_2\text{SO}_4$  (100 mg,  $0.57 \text{ mmol}$ ) was added to the solution and the precipitate ( $\text{BaSO}_4$ ) was removed. Small portions of  $\text{K}_2\text{CO}_3$  powder were then added to the solution until a pH of 6.0 was reached. The water was removed by evaporation and the white residue ( $[\text{K}_8(\mathbf{1})]$ ) was collected.  $\text{D}_2\text{O}$  (5 mL) was added to the dry residue and the solution was divided into five aliquots. Two different potential guests (0.010 mL of each) were added to each of the aliquots and the solutions were capped and stirred for 30 min.  $\text{CoCl}_2 \cdot 6\text{H}_2\text{O}$  (5.0 mg,  $21 \mu\text{mol}$ ) was added to each aliquot and the solutions stirred for 5 min, after which they were filtered and analyzed by performing proton NMR spectroscopy. The NMR peaks from encapsulated guest molecules were integrated, and a mole-to-mole ratio of encapsulated guest molecules was calculated. The selectivity ratios have an error of less than ten percent, which is due to the ability to integrate the NMR signals. To check for reproducibility, more than one run was performed with the same two guests, and most of the guests were run with benzene. In the cases of anisole and *p*-xylene, 0.0010 mL was used instead of 0.010 mL, due to their high selectivity. Due to its low selectivity, 0.010 mL of methylene chloride was run with 0.0010 mL of chloroform. The encapsulation preferences shown in Table 1 were calculated by dividing the molar encapsulation ratio of  $\text{cage-A}_{\text{guest}}/\text{cage-B}_{\text{guest}}$  by the mole ratio of  $\text{A}_{\text{guest}}/\text{B}_{\text{guest}}$  that was originally present in the solution. To calculate the encapsulation preferences, cages containing one guest were compared with cages containing the other guest.

**Titration calorimetry:** Compound **1** was formed by dissolving  $[\text{Ba}_4(\mathbf{1})]$  in HCl (1 M), followed by addition of aqueous KOH to adjust the pH of the solution to 2.0. This induced the precipitation of **1** as a white solid  $[\text{K}_{4-x}\text{H}_{4+x}(\mathbf{1})]$ , which was isolated and dried. The exact molecular weight of  $[\text{K}_{4-x}\text{H}_{4+x}(\mathbf{1})]$  was established by dissolving a known amount of it and a reference compound in  $\text{D}_2\text{O}$  and comparing the integrated  $^1\text{H}$  NMR resonances. A  $2.4 \mu\text{M}$  solution of **1** was prepared and adjusted to pH 3.0 by adding aqueous NaOH. A sample (1 mL) of this solution was placed in the calorimeter ampule along with  $\text{CoCl}_2 \cdot 6\text{H}_2\text{O}$  (2.0 mg,  $8.4 \mu\text{mol}$ ), in either the absence of guest or the presence of  $41 \mu\text{mol}$  of guest. The ampule was placed in the calorimeter and the solution was stirred (450 rpm) while the instrument equilibrated. During the titration, 40 or 50 injections of aqueous NaOH (92 mM), each with a volume of 5 or  $4 \mu\text{L}$ , were added. Heats of dilution were small compared to the heats of reaction. The results of at least six injections were averaged to calculate the heat during cage formation. The studies with benzyliminodiacetic acid were performed by using a  $9.6 \mu\text{M}$  BIDA solution.

## Acknowledgements

We thank Brigham Young University for financial support. We thank Dr. Yohgkui Zhou for the preparation of  $[\text{Ba}_4(\mathbf{1})]$ .

- [1] G. W. Gokel, *Comprehensive Supramolecular Chemistry, Vol. 1*, Pergamon, Oxford, 1996.
- [2] F. Hof, S. L. Craig, C. Nuckolls, J. Rebek, Jr., *Angew. Chem.* **2002**, *114*, 1556–1578; *Angew. Chem. Int. Ed.* **2002**, *41*, 1488–1508.
- [3] S. Leininger, B. Olenyuk, P. J. Stang, *Chem. Rev.* **2000**, *100*, 853–908.
- [4] a) T. D. Hamilton, G. S. Papaefstathiou, L. R. MacGillivray, *J. Am. Chem. Soc.* **2002**, *124*, 11606–11607; b) R.-D. Schnebeck, E. Freisinger, F. Glahe, B. Lippert, *J. Am. Chem. Soc.* **2000**, *122*, 1381–1390; c) S. Mann, G. Huttner, L. Zsolnai, K. Heinze, *Angew. Chem.* **1996**, *108*, 2983–2984; *Angew. Chem. Int. Ed. Engl.* **1996**, *35*, 2808–2809.
- [5] a) F. A. Cotton, P. Lei, C. Lin, C. A. Murillo, X. Wang, S.-Y. Yu, Z.-X. Zhang, *J. Am. Chem. Soc.* **2004**, *126*, 1518–1525; b) J.-P. Bourgeois, M. Fujita, M. Kawano, S. Sakamoto, K. Yamaguchi, *J. Am. Chem. Soc.* **2003**, *125*, 9260–9261; c) D. W. Johnson, K. N. Raymond, *Inorg. Chem.* **2001**, *40*, 5157–5161; d) A. Ikeda, H. Udzu, Z. Zhong, S. Shinkai, S. Sakamoto, K. Yamaguchi, *J. Am. Chem. Soc.* **2001**, *123*, 3872–3877; e) R. W. Saalfrank, R. Burak, S. Reihls, N. Low, F.

- Hampel, H.-D. Stachel, J. Lentmaier, K. Peters, E.-M. Peters, H. G. von Schnering, *Angew. Chem.* **1995**, *107*, 1085–1087; *Angew. Chem. Int. Ed. Engl.* **1995**, *34*, 993–995.
- [6] a) D. L. Reger, R. F. Semeniuc, M. D. Smith, *Inorg. Chem.* **2003**, *42*, 8137–8139; b) W.-Y. Sun, T. Kusukawa, M. Fujita, *J. Am. Chem. Soc.* **2002**, *124*, 11570–11571; c) S. R. Seidel, P. J. Stang, *Acc. Chem. Res.* **2002**, *35*, 972–983; d) M. Fujita, K. Umemoto, M. Yoshizawa, N. Fujita, T. Kusukawa, K. Biradha, *Chem. Commun.* **2001**, 509–518; e) H.-K. Liu, W.-Y. Sun, D.-J. Ma, K.-B. Yu, W.-X. Tang, *Chem. Commun.* **2000**, 591–592; f) S.-Y. Yu, T. Kusukawa, K. Biradha, M. Fujita, *J. Am. Chem. Soc.* **2000**, *122*, 2665–2666; g) B. F. Abrahams, S. J. Egan, R. Robson, *J. Am. Chem. Soc.* **1999**, *121*, 3535–3536; h) B. Olenyuk, M. D. Levin, J. A. Whiteford, J. E. Shield, P. J. Stang, *J. Am. Chem. Soc.* **1999**, *121*, 10434–10435; i) T. Kusukawa, M. Fujita, *Angew. Chem.* **1998**, *110*, 3327–3329; *Angew. Chem. Int. Ed.* **1998**, *37*, 3142–3144.
- [7] a) S. J. Park, J. W. Lee, S. Sakamoto, K. Yamaguchi, J.-I. Hong, *Chem. Eur. J.* **2003**, *9*, 1768–1774; b) F. Fochi, P. Jacopozzi, E. Wegeilius, K. Rissanen, P. Cozzini, E. Marastoni, E. Fiscaro, P. Manini, R. Fokkens, E. Dalcanale, *J. Am. Chem. Soc.* **2001**, *123*, 7539–7552; c) O. D. Fox, M. G. B. Drew, P. D. Beer, *Angew. Chem.* **2000**, *112*, 139–144; *Angew. Chem. Int. Ed.* **2000**, *39*, 136–139; d) O. D. Fox, N. K. Dalley, R. G. Harrison, *Inorg. Chem.* **1999**, *38*, 5860–5862; e) O. D. Fox, N. K. Dalley, R. G. Harrison, *J. Am. Chem. Soc.* **1998**, *120*, 7111–7112.
- [8] O. D. Fox, J. F. Leung, J. M. Hunter, N. K. Dalley, R. G. Harrison, *Inorg. Chem.* **2000**, *39*, 783–790.
- [9] a) D. A. Makeiff, J. C. Sherman, *Chem. Eur. J.* **2003**, *9*, 3253–3262; b) D. A. Makeiff, D. J. Pope, J. C. Sherman, *J. Am. Chem. Soc.* **2000**, *122*, 1337–1342; c) R. G. Chapman, J. C. Sherman, *J. Org. Chem.* **1998**, *63*, 4103–4110; d) R. G. Chapman, N. Chopra, E. D. Cochein, J. C. Sherman, *J. Am. Chem. Soc.* **1994**, *116*, 369–370.
- [10] a) K. Kobayashi, K. Ishii, S. Sakamoto, T. Shirasaka, K. Yamaguchi, *J. Am. Chem. Soc.* **2003**, *125*, 10615–10624; b) F. Hof, C. Nuckolls, J. Rebek, Jr., *J. Am. Chem. Soc.* **2000**, *122*, 4251–4252; c) M. C. Calama, P. Timmerman, D. N. Reinhoudt, *Angew. Chem.* **2000**, *112*, 771–774; *Angew. Chem. Int. Ed.* **2000**, *39*, 755–758; d) M. Fujita, S. Nagao, K. Ogura, *J. Am. Chem. Soc.* **1995**, *117*, 1649–1650.
- [11] a) S. Hiraoka, M. Fujita, *J. Am. Chem. Soc.* **1999**, *121*, 10239–10240; b) J. S. Fleming, K. L. V. Mann, C.-A. Carraz, E. Psillakis, J. C. Jeffery, J. A. McCleverty, M. D. Ward, *Angew. Chem.* **1998**, *110*, 1315–1318; *Angew. Chem. Int. Ed.* **1998**, *37*, 1279–1281.
- [12] a) S. M. Biros, E. C. Ullrich, F. Hof, L. Trembleau, J. Rebek, Jr., *J. Am. Chem. Soc.* **2004**, *126*, 2870–2876; b) Z. R. Laughrey, C. L. D. Gibb, T. Senechal, B. C. Gibb, *Chem. Eur. J.* **2003**, *9*, 130–139; c) F. Hof, L. Trembleau, E. C. Ullrich, J. Rebek, Jr., *Angew. Chem.* **2003**, *115*, 3258–3261; *Angew. Chem. Int. Ed.* **2003**, *42*, 3150–3153; d) F. Corbellini, R. Fiammengo, P. Timmerman, M. Crego-Calama, K. Versluis, A. J. R. Heck, I. Luyten, D. N. Reinhoudt, *J. Am. Chem. Soc.* **2002**, *124*, 6568–6575; e) J. M. Rivera, T. Martín, J. Rebek, Jr., *J. Am. Chem. Soc.* **2001**, *123*, 5213–5220; f) A. Shivanyuk, J. Rebek, Jr., *Chem. Commun.* **2001**, 2424–2425; g) T. Heinz, D. M. Rudkevich, J. Rebek, Jr., *Angew. Chem.* **1999**, *111*, 1206–1209; *Angew. Chem. Int. Ed.* **1999**, *38*, 1136–1139; h) T. Heinz, D. M. Rudkevich, J. Rebek, Jr., *Nature*, **1998**, *394*, 764–766.
- [13] a) D. Fiedler, D. H. Leung, R. G. Bergman, K. N. Raymond, *J. Am. Chem. Soc.* **2004**, *126*, 3674–3675; b) T. Kusukawa, M. Fujita, *J. Am. Chem. Soc.* **1999**, *121*, 1397–1398; c) T. N. Parac, D. L. Caulder, K. N. Raymond, *J. Am. Chem. Soc.* **1998**, *120*, 8003–8004.
- [14] a) G. L. Amidon, S. H. Yalkowsky, S. Leung, *J. Pharm. Sci.* **1974**, *63*, 1858–1866; b) C. McAuliffe, *Nature* **1963**, *200*, 1092–1093.
- [15] a) Y. Zhang, S. Akilesh, D. E. Wilcox, *Inorg. Chem.* **2000**, *39*, 3057–3064; b) E. L. Piatnitshki, R. A. Flowers, K. Deshayes, *Chem. Eur. J.* **2000**, *6*, 999–1006; c) S. M. Trzaska, E. J. Toone, A. L. Crumbliss, *Inorg. Chem.* **2000**, *39*, 1071–1075.
- [16] The  $pK_a$  values of **1** may be different from the quoted literature values, due to the proximity of the iminodiacetate groups on the resorcinarene. However, pH titrations of **1** give  $pK_a$  values close to the literature values of iminodiacetic acid. See: L. G. Sillén, A. E. Martell, *Stability Constants of Metal-Ion Complexes, Supplement No 1*, The Chemical Society, Burlington House, London, **1971**.
- [17] D. J. Eatough, E. A. Lewis, L. D. Hansen in *Analytical Solution Calorimetry* (Ed.: J. K. Grime), Wiley, New York, **1985**, pp. 137–161. The conditional equilibrium constant is based on each IDA amine unit being a monoprotic acid. This assumption seems to be validated by the similarity between our values and the literature values.
- [18] K. T. Holman in *Encyclopedia of Supramolecular Chemistry* (Eds.: J. L. Atwood, J. W. Steed), Marcel Dekker, New York, **2004**, pp. 340–348.
- [19] a) R. Warmuth, M. A. Marvel, *Chem. Eur. J.* **2001**, *7*, 1209–1220; b) A. R. Renslo, F. C. Tucci, D. M. Rudkevich, J. Rebek, Jr., *J. Am. Chem. Soc.* **2000**, *122*, 4573–4582.

Received: March 17, 2005

Published online: June 23, 2005